Journal of Nuclear Medicine, published on December 13, 2019 as doi:10.2967/jnumed.119.236786

Radiation dosimetry and biodistribution of ^{68}Ga-FAPI-46 PET imaging in cancer patients

Authors List:

Catherine Meyer[1,2], Magnus Dahlbom[1,2], Thomas Lindner[3], Sebastien Vauclin[4], Christine Mona[2], Roger Slavik[1,2,5], Johannes Czernin[2,6,7], Uwe Haberkorn[3,7,8], Jeremie Calais[1,2,5,6].

Affiliations:

1. Physics & Biology in Medicine Interdepartmental Graduate Program, David Geffen School of Medicine, University of California Los Angeles, CA, USA.
2. Ahmanson Translational Theranostics Division, Department of Molecular & Medical Pharmacology, University of California Los Angeles, CA, USA.
3. Department of Nuclear Medicine, University Hospital Heidelberg, Germany.
4. DOSIsoft SA, Cachan, France.
5. Jonsson Comprehensive Cancer Center, University of California Los Angeles, CA, USA.
6. Institute of Urologic Oncology, University of California Los Angeles, CA, USA.
7. Clinical Cooperation Unit Nuclear Medicine, DKFZ Heidelberg, Germany.
8. Translational Lung Research Center Heidelberg (TLRC), German Center for Lung Research (DZL), Heidelberg, Germany.

First author:

Catherine Meyer
In training (Student)
Ahmanson Translational Theranostics Division,
Department of Molecular and Medical Pharmacology,
David Geffen School of Medicine,
University of California Los Angeles,
200 Medical Plaza, Suite B114-61,
Los Angeles, CA 90095
Phone: 310-825-4321
E-mail: cameyer@mednet.ucla.edu

Corresponding Author:

Jeremie Calais, MD MSc
Ahmanson Translational Theranostics Division,
Department of Molecular and Medical Pharmacology,
David Geffen School of Medicine,
University of California Los Angeles,
200 Medical Plaza, Suite B114-61,
Los Angeles, CA 90095
Phone: 310-825-3617
E-mail: jcalais@mednet.ucla.edu

Short title:

68Ga-FAPI-46 dosimetry

Key words:

FAPI; PET/CT; Gallium-68; dosimetry; biodistribution

Financial Disclosure

JCa is consultant for Blue Earth Diagnostics, Progenics Radiopharmaceuticals and Radiomedix, outside of the submitted work. JCz is a co-founder and holds equity in Sofie Biosciences and Trethera Therapeutics. Intellectual property patented by the University of California has been licensed to Sofie Biosciences and Trethera Therapeutics. This intellectual property was not used in the current study. SV is an employee of DOSIsoft SA (Cachan, France). UH and TL are co-authors on a patent application for FAP agents. No other potential conflict of interest relevant to this article was reported.

Word count: 4670

ABSTRACT

Background. Targeting cancer-associated fibroblasts (CAFs) has become an attractive goal for diagnostic imaging and therapy as they can constitute as much as 90% of tumor mass. The serine protease fibroblast activation protein (FAP) is overexpressed selectively in CAFs, drawing interest in FAP as a stromal target. The quinoline-based FAP-inhibitor PET tracer, ^{68}Ga-FAPI-04, has been previously shown to yield high tumor-to-background ratios (TBR) in patients with various cancers. Recent developments towards an improved compound for therapeutic application have identified FAPI-46 as a promising agent due to a longer tumor retention time in comparison with FAPI-04. Here we present a PET biodistribution and radiation dosimetry study of ^{68}Ga-FAPI-46 in cancer patients. **Methods.** Six patients with different cancers underwent serial ^{68}Ga-FAPI-46 PET/CT scans at three time points following radiotracer injection: 10 minutes, 1 hour, and 3 hours. The source organs consisted of the kidneys, bladder, liver, heart, spleen, bone marrow, uterus, and body remainder. OLINDA/EXM v.1.1 software was used to fit and integrate the kinetic organ activity data to yield total body and organ time-integrated activity coefficients/residence times and finally organ absorbed doses. Standardized uptake values (SUV) and TBR were generated from the contoured tumor and source organ volumes. Spherical volumes in muscle and blood pool were also obtained for TBR (Tumor SUVmax / Organ SUVmean). **Results**. At all timepoints, the highest organ SUVmax was observed in the liver. Tumor and organ mean SUVs decreased whereas TBRs in all organs but the uterus increased with time. Organs with the highest effective doses were the bladder wall (2.41E-03 mSv/MBq), followed by ovaries (1.15E-03 mSv/MBq) and red marrow (8.49E-04mSv/MBq). The average effective total body dose was 7.80E-03 mSv/MBq. **Conclusion.** ^{68}Ga-FAPI-46 PET/CT has a favorable dosimetry profile with an estimated whole body dose of 5.3 mSv for an administration of 200 MBq (5.4 mCi) of ^{68}Ga-FAPI-46 (1.56± 0.26 mSv from the PET tracer and 3.7 mSv from one low-dose CT scan). The biodistribution study showed high TBRs increasing

over time, suggesting high diagnostic performance and favorable tracer kinetics for potential therapeutic applications.

INTRODUCTION

Targeting the stroma in the tumor microenvironment has become an attractive goal for diagnostic imaging and therapy (*1-3*). Cancer-associated fibroblasts (CAFs) are the predominant component of the stroma surrounding epithelial cancer cells, and they can comprise up to 90% of the total tumor mass in desmoplastic cancers (*4-7*). These reactive stromal cells selectively produce fibroblast activation protein (FAP), a serine protease which is scarcely expressed within the stroma of healthy tissues (*1,4,5*). FAP-positive CAFs are reported to promote and enhance pro-tumorigenic characteristics such as angiogenesis, neoplastic progression, metastatic invasion and migration (*4,8-14*). FAP expression is high in CAFs, but low in normal adult tissues, except for sites of active tissue damage, remodeling and inflammation (*4*).

The specificity of FAP for the CAFs in the tumor microenvironment provided the motivation to develop FAP-specific small molecule inhibitors. Several quinoline-based FAP-inhibitors labeled with positron emitters have been developed (*15-17*). Most recently, FAPI-04 labeled with ^{68}Ga provided PET images with high tumor-to-background ratios (TBRs) in patients across a wide array of cancers, suggesting high potential for FAP-targeted diagnostics, and possibly molecular radiotherapy (*17-20*). Because the stroma can represent up to 90% of the total tumor mass, stroma-targeted PET imaging may be more sensitive than glucose metabolism PET imaging for tumor detection in some cancers (*16,18,21,22*). In the context of stroma-targeted radionuclide therapy, breaking the tumor stroma barrier may increase tumor cells accessibility for pharmacologic, immunologic or cell based therapies (10-12). Additionally, delivery of ionizing radiation to the cancer cells may also be possible by crossfire effect.

In an effort to increase FAPI tumor uptake and retention for therapeutic applications, related FAPI-04 derivatives were previously developed and assessed preclinically as well as in cancer patients (*17*). From these studies, FAPI-46 emerged as the most promising tracer for therapeutic clinical

application due to its high tumor uptake and retention, and lower uptake in normal organs compared with FAPI-04. As a required step for further translation and approval by regulatory agencies, the primary objective of this study was to provide the radiation dosimetry analysis in cancer patients who underwent ^{68}Ga-FAPI-46 PET imaging. The secondary aim was to describe the organ biodistribution, SUV metrics, and temporal changes in TBR values (Tumor SUVmax / Organ SUVmean).

MATERIALS AND METHODS

Study Design and Patients

This is a retrospective study of radiation dosimetry and biodistribution of a novel PET imaging probe. The imaging data acquisition was performed at the Heidelberg University Hospital in Germany. The analysis was conducted at the University of California Los Angeles, USA. Six patients (4 males, 2 females; age 56 – 81 years) with different cancer types were included. All six patients were referred for an unmet diagnostic challenge that could not be solved sufficiently with standard diagnostic imaging. A summary of patient characteristics is presented in Table 1. All patients gave written informed consent to receive FAPI PET/CT. Following the regulations of the German Pharmaceuticals Act §13(2b), indication and labeling of the FAPI-tracers were conducted under the direct responsibility of the applying physician. The data were analyzed retrospectively with approval of the local ethics committee (No. S016/2018).

Radiopharmaceutical Synthesis

The radiotracer synthesis was conducted as previously described (*15-17*). Briefly, radiolabeling was performed by adjusting a mixture of 20 nmol FAPI-46, 10 µL ascorbic acid solution (20% in water) and 1 mL ^{68}Ga-solution (0.6-2 GBq in 0.6 M HCl in water) to pH 3.3-3.6 with sodium acetate (2.5 M in water). After heating to 95 °C for 20 minutes, the product was isolated by solid phase extraction (Oasis

light HLB, Waters) using 0.5 mL ethanol as eluent. After dilution with 5 mL sodium chloride solution (0.9%) the pH was adjusted to pH 7 by addition of phosphate buffer.

PET/CT Image Acquisition

Injected activity was limited to 100-370 MBq per exam based on previous dosimetry estimates of related FAP inhibitors with an effective whole body dose of 1.6 mSv/100 MBq as well as count rate considerations (*21*). Each patient underwent PET/CT imaging scans at three time points after radiotracer injection: 10 minutes (prior to voiding), 1 hour, and 3 hours. No bladder voiding model was used and thereby the calculated bladder dose will be the maximum dose assuming no voiding. All imaging was performed on a Biograph mCT Flow scanner (Siemens, Erlangen, Germany). Following non-contrast-enhanced low-dose CT (130keV, 30mAs, CareDose; reconstructed with a soft tissue kernel to a slice thickness of 5mm, increment of 3-4 mm), PET images were acquired in 3-D mode (matrix 200 × 200) using FlowMotion™ (Siemens) with 0.7 cm/min continuous bed motion. The emission data were corrected for randoms, scatter and decay. Reconstruction was performed with an ordered subset expectation maximization (OSEM) algorithm with 2 iterations / 21 subsets and Gauss-filtered to a transaxial resolution of 5 mm at full-width at half-maximum; Attenuation correction was performed using the non-enhanced low dose CT data.

Radiation Dosimetry

Mean absorbed radiation doses were estimated using the source and target organ framework outlined by the Medical Internal Radiation Dose (MIRD) Committee (*23,24*). Organ delineation and activity accumulation at each imaging time point was calculated using PLANET® Dose internal dosimetry software (DOSIsoft SA, Cachan, France). Time-activity curve fitting and subsequent dose calculation was performed using OLINDA/EXM v.1.1. The source organs consisted of the kidney parenchyma, urinary bladder, liver, heart contents, spleen, bone marrow, uterus, as well as body remainder. Source organs were chosen based on highest tracer uptake and previously published work (*21*).

Source organ volumes of interest (VOIs) were contoured manually (CM, JCa) at the first time point and propagated to later time point scans based on automatic deformable registration between each scan. Propagated organ volumes were then manually adjusted when necessary (CM, JCa). Organ volume differences that arose due to elastic propagation between time points were accounted for by calculating the mean volume for organ mass input for dose calculation in OLINDA/EXM. Kidney volumes included left and right renal parenchyma, excluding the urinary activity in renal calyces, as shown in Figure 1. The urinary activity (Figure 1, Panel B) was delineated using SUV thresholding and subsequently subtracted from the entire kidney volume to yield only kidney parenchyma (Figure 1, Panel C). Activity in the bone marrow was determined by contouring two lumbar vertebrae and scaling based on the proportion of total body bone marrow mass, with each vertebra assumed to contain 2.5% (*25*).

In all cases, tumor lesion activity was excluded from normal organ source volumes by Boolean subtraction operations and incorporated in the body remainder term. Tumors were contoured (CM, JCa) using patient-specific SUV thresholding with manual adjustment (SUV threshold ranged from 2.5-3.5). The body remainder volume was determined by subtracting all source organs from a whole-body contour.

Following tumor and organ contouring, the non-decay-corrected percent injected activity accumulated in the organs at each time point per patient was then used as input for OLINDA/EXM v.1.1 software. Patient-specific masses were used for the liver, kidneys, spleen, uterus, and total body. The organ and total body/remainder activity kinetic data were then fitted with a monoexponential decay function using OLINDA/EXM v.1.1. Representative percent injected activity curves for various source organs for one patient are shown in Figure 2. The functions are integrated to obtain time-integrated activity coefficients and S-values are applied according to MIRD methodology from standard adult phantoms to yield absorbed and effective radiation doses. Radiation weighting factors from ICRP 60 were applied for calculation of effective doses (*26*). The calculated doses based on individual patient

inputs were then reported as means ± SD to more accurately represent the general population risk associated with this imaging scan.

Biodistribution

In addition to the contoured tumor and source organ volumes drawn for dosimetry, spherical volumes in the gluteal muscle (range 7-20 mL) and blood pool in the ascending aorta (range 4-5 mL) were created and automatically propagated to later time points for biodistribution analysis. Mean and maximum standardized uptake values (SUV) were generated for all previously contoured organs and spherical muscle and blood VOIs to compute TBRs (Tumor SUVmax / Organ SUVmean).

RESULTS

PET/CT Imaging

The injected activity of ^{68}Ga-FAPI-46 ranged from 214-246 MBq (5.8 – 6.6 mCi) (Table 1). Images were acquired at 12 ± 2.5 minutes, 1.2 ± 0.3 hours, and 3.3 ± 0.3 hours after intravenous administration of ^{68}Ga-FAPI-46. The tracer injection was well tolerated without any side effects in all 6 patients. No adverse events were observed during the three hours following injection. Maximum intensity projections (MIPs) and organ volumes used for activity quantification are shown for Patient 3 (female) and Patient 5 (male) in Figures 3 and 4, respectively. The other patients' images and SUV kinetics are available in supplemental Figures 1-4.

Radiation Dosimetry

The monoexponential curve fitting parameters and time-integrated activity coefficients (residence times) for each source organ are summarized in Table 2. The pooled patient dosimetry reports from OLINDA/EXM v.1.1 are shown in Table 3.

The organ with the highest absorbed dose was the urinary bladder wall with 4.83E-02 mGy/MBq, followed by the kidneys (1.60E-02 mGy/MBq), the heart wall (1.11E-02 mGy/MBq), liver (1.01E-02 mGy/MBq), and the uterus (9.54E-03 mGy/MBq). The remaining organ absorbed doses were

all below 6.96E-03 mGy/MBq. Organs with the highest effective doses were the bladder wall (2.41E-03 mSv/MBq), followed by ovaries (1.15E-03 mSv/MBq) and red marrow (8.49E-04mSv/MBq). The average total body absorbed dose was 5.82E-03 mGy/MBq and the effective dose was 7.80E-03 mSv/MBq - similar, though lower than the reported values for related FAP-inhibitors (*21*). Thus for administration of 200 MBq (5.4 mCi) ^{68}Ga-FAPI-46 the total body effective dose was 1.56 mSv ± 0.26 mSv. Together with approximately 3.7 mSv from one low-dose CT attenuation scan (*27*), this results in an estimated total effective dose of 5.3 mSv. Reported standard deviations arise from calculating the mean OLINDA/EXM v.1.1 dosimetry profile from six patients, and does not account for any possible errors involved in organ delineation.

Biodistribution

Biodistribution data assessed by SUV kinetics for Patient 3 (female) and Patient 5 (male) are shown in Figures 3 and 4, respectively. Pooled SUVmax and TBRs for all six patients are summarized in Figure 5; SUVmean are listed in Table 4. The highest average normal organ SUVmax at all time points was observed in the liver, decreasing from an average SUVmax of 7.4 at 10 minutes to 5.0 by 3.3 hours (decline of 32%). Tracer uptake in the tumor was rapid with greater retention than normal organs: average SUVmax of 15.5 at 10 minutes, and 13.4 at 3.3 hours (decrease of 14%).

Tumor and organ mean SUVs decreased in all patients from the first to last time points, while TBRs increased with time (with the exception of the uterus TBR). The highest TBR at all timepoints was observed in the marrow, with a ratio of 31 at 3.3 hours. The tumor-to-muscle ratio of 10.7 at 10 minutes increased more than 2-fold at 3.3 hours to 22.8. At 3.3 hours, the next highest TBRs were observed in the heart (19.1), spleen (18.9) and liver (16.8).

In summary, the tracer rapidly accumulated in the primary tumors and metastases with high maximum SUVs and low tracer uptake in normal tissue. The radioactivity was cleared steadily from the blood pool and was excreted via the kidneys, producing high contrast images.

DISCUSSION

Herein we describe the biodistribution of ^{68}Ga-FAPI-46 and its estimated radiation dose deposition in organs of six cancer patients who underwent ^{68}Ga-FAPI-46 PET/CT imaging at three time points. These are required for clinical translation and approval by regulatory agencies. The average effective whole-body dose for administration of 200 MBq ^{68}Ga was 1.56 ± 0.26 mSv (7.80E-03 ± 1.31E-03 mSv/MBq). This estimate is slightly lower than the prior reported effective total body effective doses of other ^{68}Ga-FAPI PET tracers: 1.80E-02 and 1.64E-02 mSv/MBq with ^{68}Ga-FAPI-02 and ^{68}Ga-FAPI-04, respectively (*21*). As a comparison, the reported effective dose for ^{68}Ga-PSMA-11 ranges from 1.08E-02 – 2.46E-02 mSv/MBq (*28,29*), while the effective total body dose of both ^{68}Ga-DOTATOC and ^{68}Ga-DOTATATE is 2.10E-02 ± 3.00E-03 mSv/MBq (*30*).

Despite collection of patient-specific time-activity curves, the dose calculation was based on the stylized phantoms provided in OLINDA/EXM v.1.1. These estimates provide generalizable population mean absorbed dose values to organs by means of standard phantoms with selected customized organ masses. The reported standard deviations for the dosimetry estimates (Table 3) arise from taking the average of six sets of OLINDA/EXM v.1.1 patient reports. There are however sources of uncertainty not included in the analysis that are inherent in the dose calculation process that propagate to the final dose result. One of the most significant contributing sources of uncertainty is the organ volume delineation itself (*31,32*). Inter-patient variability is also seen within Table 2 which shows relatively high standard deviations for time-activity curve-fitting parameters, most prominently observed in the liver.

While tumor dosimetry was not addressed directly in this study, the trend in biodistribution observed up to 3.3 hours after tracer administration demonstrates rapid tumor uptake and satisfactory retention. FAPI-46 biodistribution and dosimetry, including tumor dosimetry, using longer-lived isotopes for therapeutic applications remains to be studied. Such studies are essential to evaluate longer term tracer kinetics and thereby determine rational therapeutic isotope conjugates with well-matched physical half-life. The promising trend observed thus far of increasing TBRs over time seems to be favorable for therapeutic applications. Given the high achieved TBRs even at 10 minutes, early timepoint imaging with ^{68}Ga-FAPI becomes possible; however, it should be considered that the contrast ratio improves with time.

This analysis was limited to six cancer patients (4 males; 2 females), and no healthy subjects. The basal FAP expression profile of a greater variety of cancers as well as in healthy subjects remains to be quantitatively assessed. It is however known that FAP is expressed at sites of arthritis, wound healing and active tissue remodeling, bone marrow mesenchymal cells, as well as in cirrhotic liver (*5,18,33,34*). The extent of this expression and its impact on imaging and potential therapies requires further clinical study. Implementation of FAP-targeted therapies thereby necessitates a better understanding of the comprehensive role of FAP, not only in the tumor microenvironment and carcinogenesis of different cancer types, but also its role in widespread bodily fibrotic mechanisms. Evaluation of ^{68}Ga-FAPI-46 diagnostic accuracy was outside the study scope.

CONCLUSION

^{68}Ga-FAPI-46 PET/CT imaging is shown to have a favorable dosimetry profile. For administration of 200 MBq (5.4 mCi) of ^{68}Ga-FAPI-46, the effective whole body dose of a PET scan is 1.56 mSv ± 0.26 mSv. When including a low dose CT (3.7 mSv), the dose of a ^{68}Ga-FAPI-46 PET/CT scan is approximately 5.3 mSv in total. The biodistribution study showed high TBRs increasing over time, suggesting high diagnostic performance and favorable tracer kinetics for potential therapeutic applications. Long-term

tracer biodistribution and dosimetry for longer-lived therapeutic isotope applications remains to be studied. Further work is needed to better identify indications for FAPI PET/CT as well as its diagnostic accuracy.

Financial Disclosure

JCa is consultant for Blue Earth Diagnostics, Progenics Radiopharmaceuticals and Radiomedix, outside of the submitted work. JCz is a co-founder and holds equity in Sofie Biosciences and Trethera Therapeutics. Intellectual property patented by the University of California has been licensed to Sofie Biosciences and Trethera Therapeutics. This intellectual property was not used in the current study. SV is an employee of DOSIsoft SA (Cachan, France). UH and TL are co-authors on a patent application for FAP agents. No other potential conflict of interest relevant to this article was reported.

KEY POINTS

QUESTION: What is the biodistribution and radiation dosimetry profile of 68Ga-FAPI-46, a new PET tracer targeting tumor stroma with high potential for theranostic applications?

PERTINENT FINDINGS: Based on three serial 68Ga-FAPI-46 PET/CT scans acquired in six cancer patients, the average effective whole-body dose estimation for administration of 200 MBq 68Ga-FAPi-46 was 1.56 mSv which is lower than with other Gallium-68 PET tracers (68Ga-PSMA-11 or 68Ga-DOTATATE). The biodistribution study showed high tumor-to-background ratios increasing over time.

IMPLICATIONS FOR PATIENT CARE: This study confirms the high potential of 68Ga-FAPI-46 for theranostic applications and provides required data for translation and approval by regulatory agencies.

REFERENCES

1. Chen X, Song E. Turning foes to friends: targeting cancer-associated fibroblasts. *Nat Rev Drug Discov.* 2019;18:99-115.

2. Katayama Y, Uchino J, Chihara Y, et al. Tumor neovascularization and developments in therapeutics. *Cancers (Basel).* 2019;11:316.

3. Weis SM, Cheresh DA. Tumor angiogenesis: molecular pathways and therapeutic targets. *Nat Med.* 2011;17:1359-1370.

4. Pure E, Blomberg R. Pro-tumorigenic roles of fibroblast activation protein in cancer: back to the basics. *Oncogene.* 2018;37:4343-4357.

5. Brennen WN, Isaacs JT, Denmeade SR. Rationale behind targeting fibroblast activation protein-expressing carcinoma-associated fibroblasts as a novel chemotherapeutic strategy. *Mol Cancer Ther.* 2012;11:257-266.

6. Garin-Chesa P, Old LJ, Rettig WJ. Cell surface glycoprotein of reactive stromal fibroblasts as a potential antibody target in human epithelial cancers. *Proc Natl Acad Sci U S A.* 1990;87:7235-7239.

7. Shiga K, Hara M, Nagasaki T, Sato T, Takahashi H, Takeyama H. Cancer-associated fibroblasts: their characteristics and their roles in tumor growth. *Cancers (Basel).* 2015;7:2443-2458.

8. Lo A, Li CP, Buza EL, et al. Fibroblast activation protein augments progression and metastasis of pancreatic ductal adenocarcinoma. *JCI Insight.* 2017;2;e92232.

9. Gao LM, Wang F, Zheng Y, Fu ZZ, Zheng L, Chen LL. Roles of fibroblast activation protein and hepatocyte growth factor expressions in angiogenesis and metastasis of gastric cancer. *Pathol Oncol Res.* 2019;25:369-376.

10. Liu J, Huang C, Peng C, et al. Stromal fibroblast activation protein alpha promotes gastric cancer progression via epithelial-mesenchymal transition through Wnt/ beta-catenin pathway. *BMC Cancer.* 2018;18:1099.

11. Jia J, Martin TA, Ye L, et al. Fibroblast activation protein-alpha promotes the growth and migration of lung cancer cells via the PI3K and sonic hedgehog pathways. *Int J Mol Med.* 2018;41:275-283.

12. Zi FM, He JS, Li Y, et al. Fibroblast activation protein protects bortezomib-induced apoptosis in multiple myeloma cells through beta-catenin signaling pathway. *Cancer Biol Ther.* 2014;15:1413-1422.

13. Zi F, He J, He D, Li Y, Yang L, Cai Z. Fibroblast activation protein alpha in tumor microenvironment: recent progression and implications (review). *Mol Med Rep.* 2015;11:3203-3211.

14. Liu F, Qi L, Liu B, et al. Fibroblast activation protein overexpression and clinical implications in solid tumors: a meta-analysis. *PLoS One.* 2015;10:e0116683.

15. Lindner T, Loktev A, Altmann A, et al. Development of quinoline-based theranostic ligands for the targeting of fibroblast activation protein. *J Nucl Med.* 2018;59:1415-1422.

16. Loktev A, Lindner T, Mier W, et al. A tumor-imaging method targeting cancer-associated fibroblasts. *J Nucl Med.* 2018;59:1423-1429.

17. Loktev A, Lindner T, Burger EM, et al. Development of novel FAP-targeted radiotracers with improved tumor retention. *J Nucl Med.* 2019;60:1421-1429.

18. Kratochwil C, Flechsig P, Lindner T, et al. (68)Ga-FAPI PET/CT: Tracer uptake in 28 different kinds of cancer. *J Nucl Med.* 2019;60:801-805.

19. Rohrich M, Loktev A, Wefers AK, et al. IDH-wildtype glioblastomas and grade III/IV IDH-mutant gliomas show elevated tracer uptake in fibroblast activation protein-specific PET/CT. *Eur J Nucl Med Mol Imaging.* 2019;46:2569-2580.

20. Giesel FL, Heussel CP, Lindner T, et al. FAPI-PET/CT improves staging in a lung cancer patient with cerebral metastasis. *Eur J Nucl Med Mol Imaging.* 2019;46:1754-1755.

21. Giesel FL, Kratochwil C, Lindner T, et al. (68)Ga-FAPI PET/CT: Biodistribution and preliminary dosimetry estimate of 2 DOTA-containing FAP-targeting agents in patients with various cancers. *J Nucl Med.* 2019;60:386-392.

22. Hamson EJ, Keane FM, Tholen S, Schilling O, Gorrell MD. Understanding fibroblast activation protein (FAP): substrates, activities, expression and targeting for cancer therapy. *Proteomics Clin Appl.* 2014;8:454-463.

23. Loevinger R, Budinger TF, Watson EE. *MIRD primer for absorbed dose calculations*. Revised Ed. New York, NY: Society of Nuclear Medicine; 1991:1-17.

24. Bolch WE, Eckerman KF, Sgouros G, Thomas SR. MIRD pamphlet No. 21: a generalized schema for radiopharmaceutical dosimetry--standardization of nomenclature. *J Nucl Med.* 2009;50:477-484.

25. Hindorf C, Glatting G, Chiesa C, Linden O, Flux G. EANM Dosimetry Committee guidelines for bone marrow and whole-body dosimetry. *Eur J Nucl Med Mol Imaging.* 2010;37:1238-1250.

26. ICRP. 1990 Recommendations of the International Commission on Radiological Protection.ICRP Publication 60. *Ann ICRP.* 1991;21:1-201.

27. Huang B, Law MW, Khong PL. Whole-body PET/CT scanning: estimation of radiation dose and cancer risk. *Radiology.* 2009;251:166-174.

28. Afshar-Oromieh A, Hetzheim H, Kubler W, et al. Radiation dosimetry of (68)Ga-PSMA-11 (HBED-CC) and preliminary evaluation of optimal imaging timing. *Eur J Nucl Med Mol Imaging.* 2016;43:1611-1620.

29. Pfob CH, Ziegler S, Graner FP, et al. Biodistribution and radiation dosimetry of (68)Ga-PSMA HBED CC-a PSMA specific probe for PET imaging of prostate cancer. *Eur J Nucl Med Mol Imaging.* 2016;43:1962-1970.

30. Sandstrom M, Velikyan I, Garske-Roman U, et al. Comparative biodistribution and radiation dosimetry of 68Ga-DOTATOC and 68Ga-DOTATATE in patients with neuroendocrine tumors. *J Nucl Med.* 2013;54:1755-1759.

31. Lassmann M, Eberlein U. The relevance of dosimetry in precision medicine. *J Nucl Med.* 2018;59:1494-1499.

32. Gear JI, Cox MG, Gustafsson J, et al. EANM practical guidance on uncertainty analysis for molecular radiotherapy absorbed dose calculations. *Eur J Nucl Med Mol Imaging.* 2018;45:2456-2474.

33. Keane FM, Yao TW, Seelk S, et al. Quantitation of fibroblast activation protein (FAP)-specific protease activity in mouse, baboon and human fluids and organs. *FEBS Open Bio.* 2013;4:43-54.

34. Yazbeck R, Jaenisch SE, Abbott CA. Potential disease biomarkers: dipeptidyl peptidase 4 and fibroblast activation protein. *Protoplasma.* 2018;255:375-386.

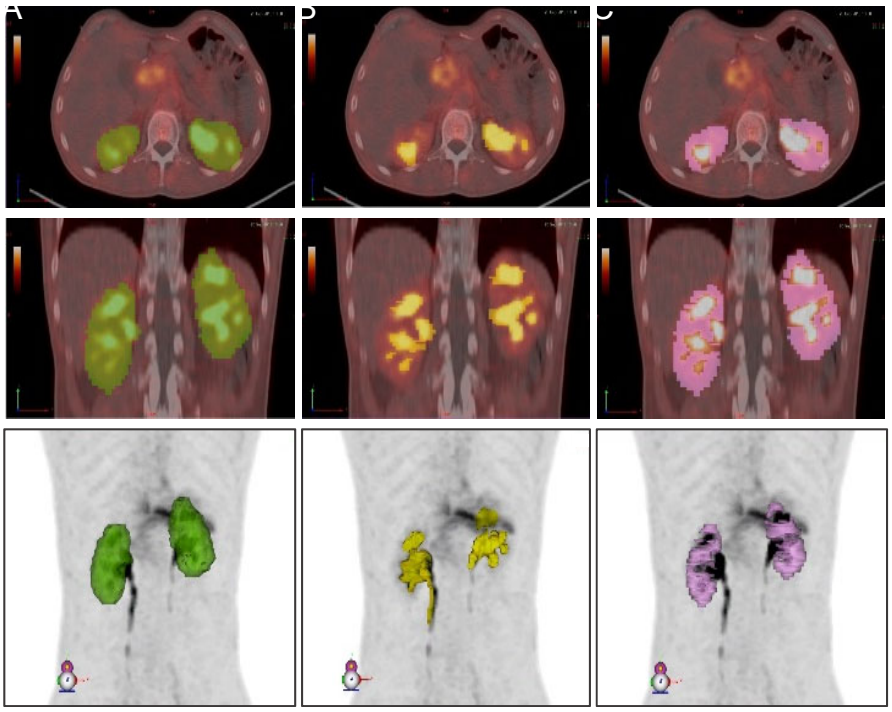

Figure 1| Delineated volumes used for determination of renal cortex volume. The entire kidney volume (Column A) from which the urine including in renal calyces is subtracted (Column B) to yield to the renal cortex volume (Column C). Images are shown for Patient 6 and are representative for the method applied for all patients. All volumes are shown in axial (top row), coronal (middle row), and MIP views (bottom row).

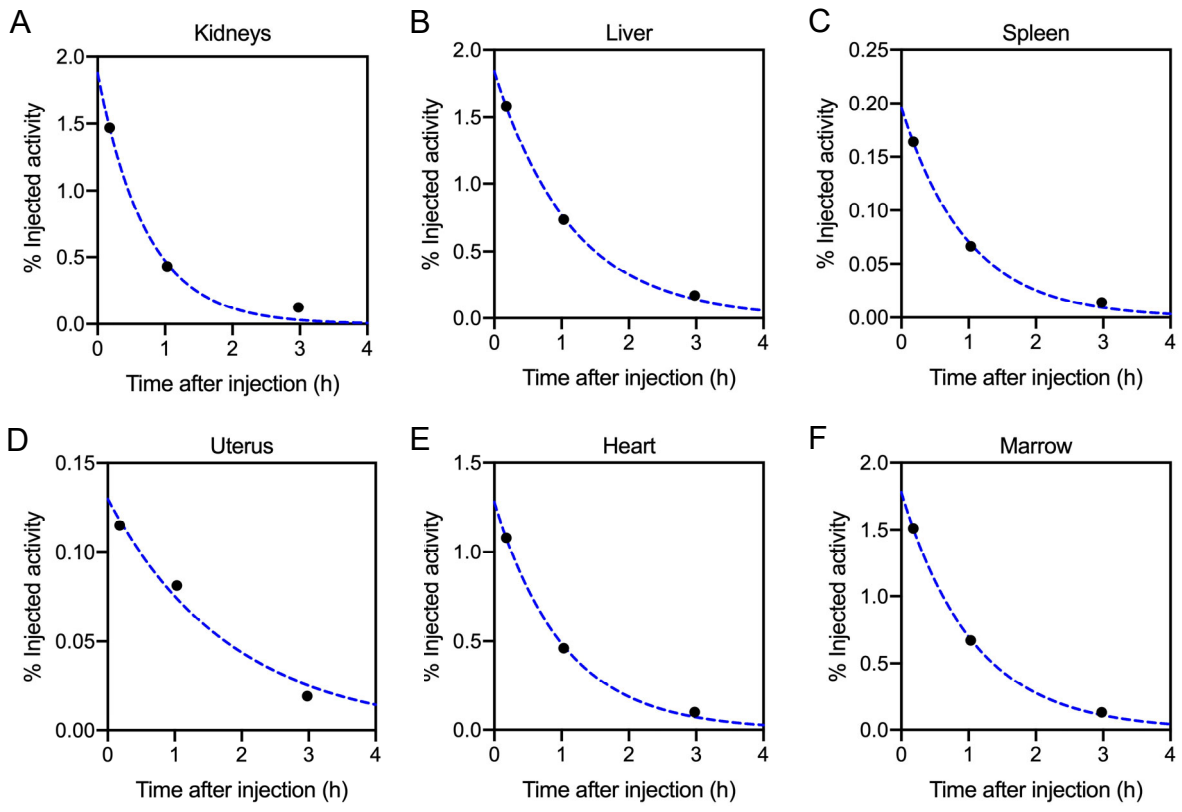

Figure 2| Percent injected activity curves for Patient 3 are shown for various source organs. The black points are the measured values and the dotted line is the monoexponential function fit to the data.

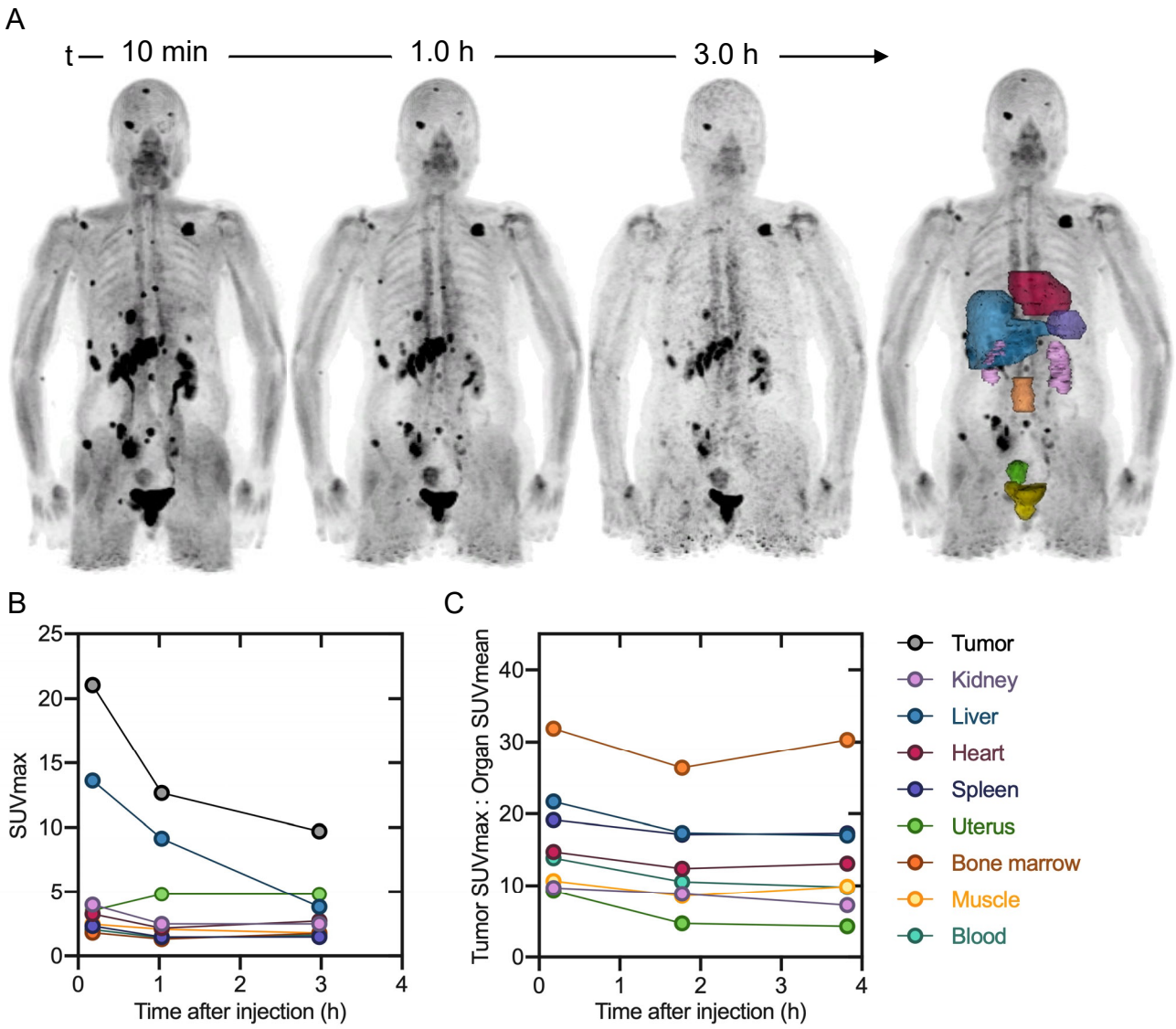

Figure 3| Patient 3 (Female) A) ^{68}Ga-FAPI-46 MIPs and delineated organs for dose calculations, B) SUVmax at three timepoints following tracer injection and C) TBR at three timepoints following tracer injection. SUVmax and TBR for the bladder are excluded from the plot. Data values available in Supplemental Table 1.

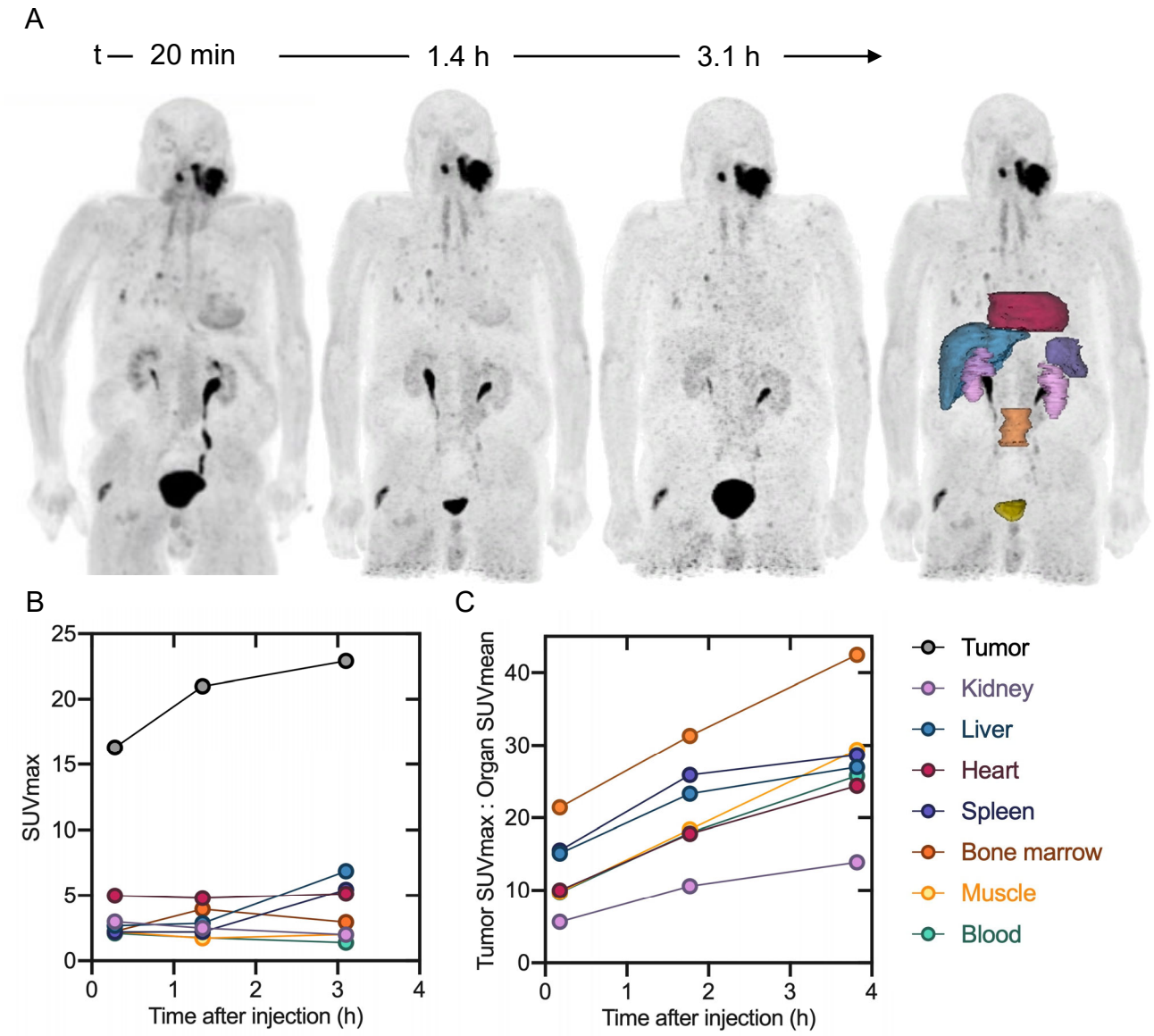

Figure 4| Patient 5 (Male) A) ^{68}Ga-FAPI-46 MIP and delineated organs for dose calculations, B) SUVmax at three timepoints following tracer injection and C) TBR at three timepoints following tracer injection. SUVmax and TBR for the bladder are excluded from the plot. Data values available in Supplemental Table 1.

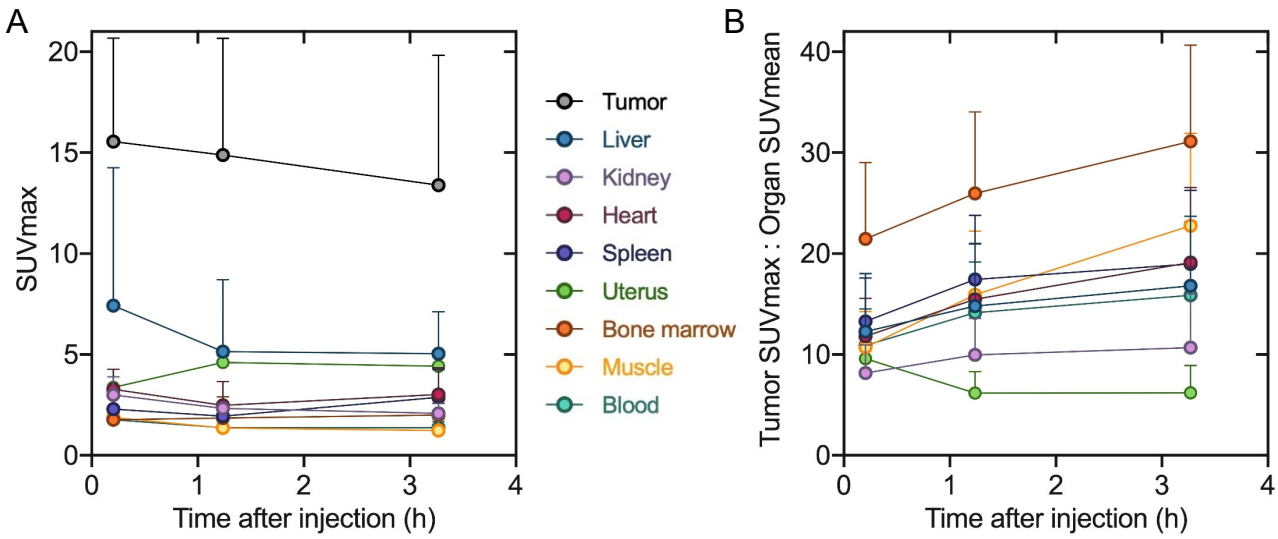

Figure 5| A) Pooled tumor and organ SUVmax and B) TBR at three timepoints following tracer injection (excluding bladder). Results are shown as mean and standard deviation for n=6 patients**.** Data values available in Table 4.

Patient no.	Sex	Age	Diagnosis	Injected activity (MBq)
1	F	63	Cholangiocellular carcinoma	246
2	M	81	Pancreatic cancer with peritonitis carcinomatosa	240
3	F	78	Breast cancer	234
4	M	56	Oropharynx carcinoma	239
5	M	78	Head and neck cancer	214
6	M	62	Gastric cancer	243

Table 1 | Patient characteristics

	$\%IA = A * \exp(-\lambda t)$		
Organ	A (%IA)	λ (h^{-1})	TIAC (h)
Liver	3.49 (2.26)	0.88 (0.12)	0.0378 (0.0198)
Kidney	2.07 (0.65)	1.08 (0.26)	0.0195 (0.0062)
Bladder	6.82 (2.32)	1.47 (0.91)	0.0595 (0.0319)
Heart	1.69 (0.30)	0.94 (0.06)	0.0182 (0.0035)
Spleen	0.71 (0.62)	0.96 (0.12)	0.0074 (0.0066)
Marrow	2.61 (0.63)	2.05 (2.97)	0.0250 (0.0114)
Uterus (n=2)	0.13 (0.004)	0.50 (0.07)	0.0027 (0.0005)

Table 2 | Monoexponential function fitting parameters and time-integrated activity coefficients (residence times) for ^{68}Ga-FAPI-46 in various organs. Results are shown as mean (standard deviation) for n=6 patients. Representative percent injected activity curves with the monoexponential curve fits overlaid are available in Supplemental Figure 1. Per-patient coefficients and TIACs are available in Supplemental Table 2.

	Dose per injected activity (mGy/MBq) (n=6) Mean (SD)	Effective dose per injected activity (mSv/MBq) (n=6) Mean (SD)
Adrenals	5.60E-03 (8.12E-04)	2.80E-05 (4.04E-06)
Brain	4.59E-03 (6.12E-04)	2.29E-05 (3.06E-06)
Breasts	4.55E-03 (6.47E-04)	2.28E-04 (3.23E-05)
Gallbladder Wall	5.62E-03 (8.53E-04)	-
LLI Wall	5.72E-03 (6.96E-04)	6.86E-04 (8.33E-05)
Small Intestine	5.48E-03 (6.37E-04)	2.74E-05 (3.20E-06)
Stomach Wall	5.32E-03 (7.25E-04)	6.38E-04 (8.69E-05)
ULI Wall	5.47E-03 (6.97E-04)	2.74E-05 (3.50E-06)
Heart Wall	1.11E-02 (1.26E-03)	-
Kidneys	1.60E-02 (4.60E-03)	7.98E-05 (2.29E-05)
Liver	1.01E-02 (7.96E-03)	5.05E-04 (4.00E-04)
Lungs	5.02E-03 (7.09E-04)	6.02E-04 (8.48E-05)
Muscle	4.96E-03 (6.54E-04)	2.48E-05 (3.27E-06)
Ovaries	5.76E-03 (6.91E-04)	1.15E-03 (1.38E-04)
Pancreas	5.69E-03 (8.49E-04)	2.84E-05 (4.24E-06)
Red Marrow	7.08E-03 (1.00E-03)	8.49E-04 (1.20E-04)
Osteogenic Cells	9.38E-03 (1.30E-03)	9.38E-05 (1.30E-05)
Skin	4.41E-03 (6.33E-04)	4.41E-05 (6.33E-06)
Spleen	6.96E-03 (2.76E-03)	3.48E-05 (1.39E-05)
Testes	4.88E-03 (6.69E-04)	1.15E-03 (1.38E-04)
Thymus	5.10E-03 (6.40E-04)	2.55E-05 (3.21E-06)
Thyroid	4.84E-03 (5.72E-04)	2.42E-04 (2.85E-05)
Urinary Bladder Wall	4.83E-02 (8.55E-03)	2.41E-03 (4.27E-04)
Uterus	9.54E-03 (5.36E-03)	4.76E-05 (2.67E-05)
Total Body	5.82E-03 (1.18E-03)	7.80E-03 (1.31E-03)
Total Body Dose for 200 MBq	1.16 mGy (0.24 mGy)	1.56 mSv (0.26 mSv)

Table 3 | ^{68}Ga-FAPI-46 dosimetry summary of mean absorbed and effective doses using OLINDA/EXM v.1.1. The effective dose in ovaries and testes are equivalent due to use of hermaphroditic adult phantom weighting. Gallbladder wall and heart wall effective doses are not available based on the ICRP radiation weighting factors. Non-pooled OLINDA/EXM v.1.1 reports, including beta and photon contribution to the total dose, are available in Supplemental Table 3.

		10 minutes	1.2 hours	3.3 hours
SUVmax tumor: SUVmean organ	T : Liver	12.28 (5.75)	14.79 (6.22)	16.80 (6.90)
	T : Kidney	8.17 (2.76)	9.96 (3.64)	10.68 (5.34)
	T : Blood	10.89 (3.61)	14.15 (5.02)	15.87 (7.30)
	T : Muscle	10.71 (3.56)	15.91 (6.33)	22.77 (9.15)
	T: Heart	11.78 (3.76)	15.48 (5.49)	19.11 (7.44)
	T : Spleen	13.27 (4.31)	17.44 (6.36)	18.99 (7.27)
	T : Marrow	21.46 (7.56)	25.96 (8.09)	31.13 (9.52)
	T: Uterus (n=2)	9.60 (0.46)	6.19 (2.12)	6.20 (2.70)
SUVmax	Tumor	15.54 (5.13)	14.89 (5.77)	13.39 (6.44)
	Liver	7.42 (6.84)	5.15 (3.56)	5.04 (2.07)
	Kidney	3.00 (0.89)	2.33 (0.26)	2.08 (0.49)
	Blood	1.77 (0.35)	1.38 (0.26)	1.37 (0.31)
	Muscle	1.87 (0.49)	1.37 (0.45)	1.24 (0.56)
	Heart	3.28 (1.00)	2.48 (1.17)	3.02 (1.31)
	Spleen	2.30 (0.23)	1.94 (0.42)	2.88 (1.38)
	Marrow	1.77 (0.34)	1.85 (1.05)	2.00 (0.59)
	Uterus (n=2)	3.37 (0.23)	4.61 (0.32)	4.42 (0.58)
SUVmean	Tumor	3.87 (1.30)	3.37 (1.11)	2.81 (1.44)
	Liver	1.51 (0.96)	1.10 (0.58)	0.81 (0.34)
	Kidney	1.92 (0.34)	1.47 (0.17)	1.25 (0.22)
	Blood	1.43 (0.25)	1.03 (0.15)	0.83 (0.15)
	Muscle	1.48 (0.41)	0.96 (0.32)	0.61 (0.24)
	Heart	1.32 (0.21)	0.95 (0.15)	0.68 (0.15)
	Spleen	1.17 (0.20)	0.85 (0.17)	0.69 (0.16)
	Marrow	0.73 (0.12)	0.56 (0.11)	0.41 (0.10)
	Uterus (n=2)	2.08 (0.27)	2.53 (0.24)	1.97 (0.42)

Table 4 | Pooled tumor to organ SUV ratios, SUVmax, and SUVmean values at three time points following ^{68}Ga-FAPI-46 administration. Results are shown as mean (standard deviation) for n=6 patients.

Radiation dosimetry and biodistribution of ^{68}Ga-FAPI-46 PET imaging in cancer patients

SUPPLEMENTAL INFORMATION

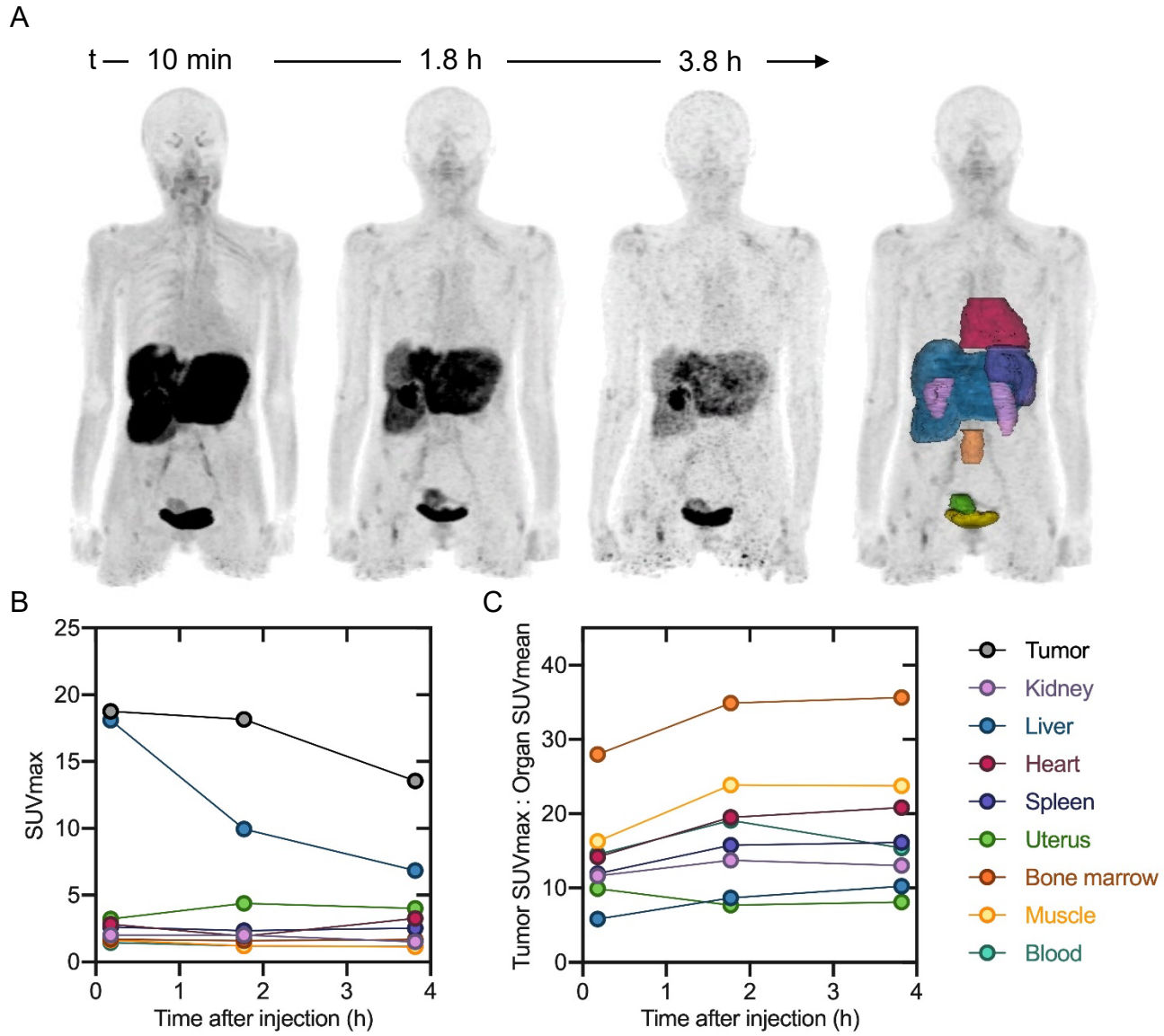

Supplemental Figure 1| Patient 1 A) ^{68}Ga-FAPI-46 MIP and delineated organs for dose calculations, B) SUVmax at three timepoints following tracer injection and C) TBR at three timepoints following tracer injection. SUVmax and TBR for the bladder are excluded from the plot. Data values available in Supplemental Table 1.

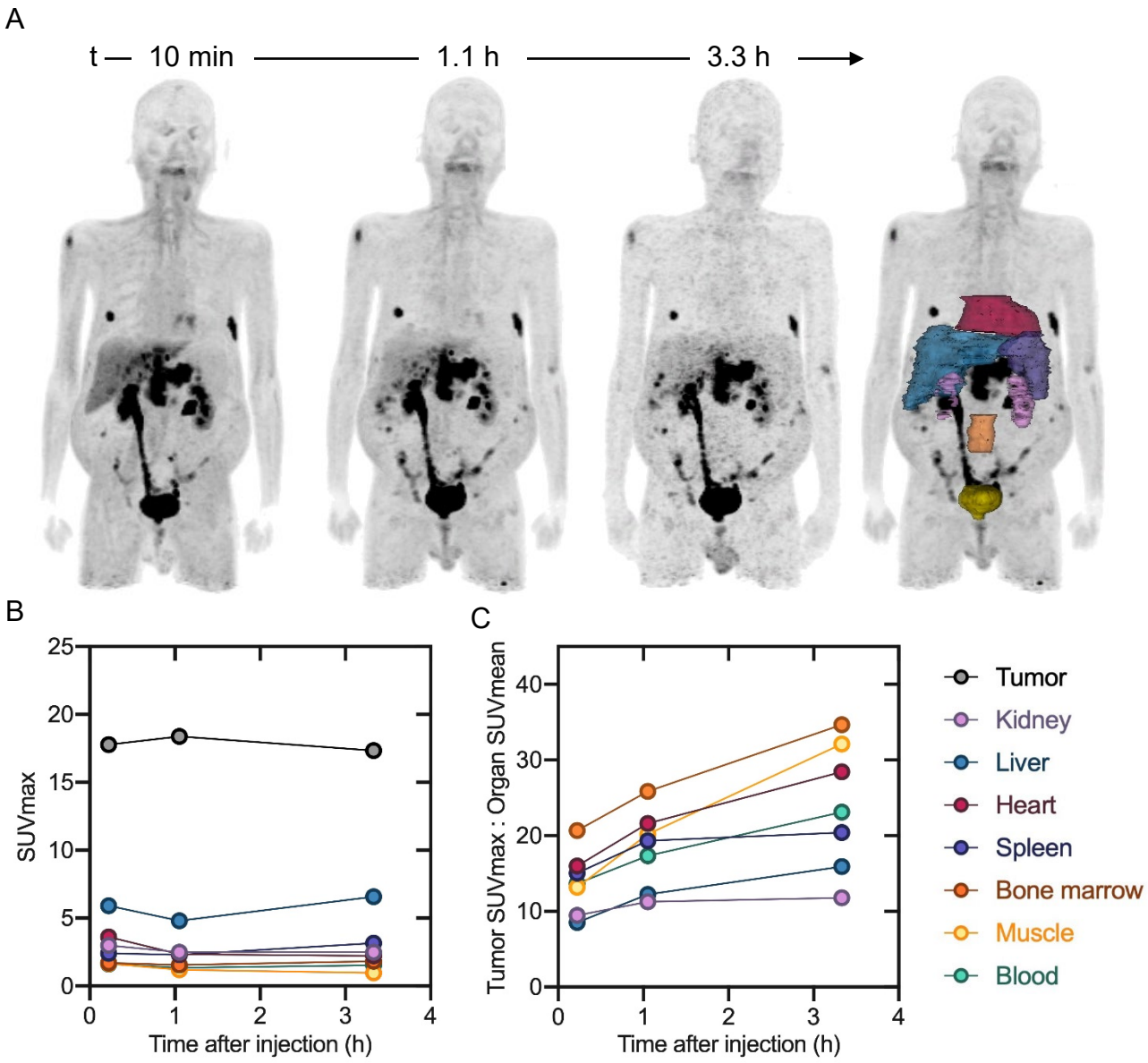

Supplemental Figure 2| Patient 2 A) ^{68}Ga-FAPI-46 MIP and delineated organs for dose calculations, B) SUVmax at three timepoints following tracer injection and C) TBR at three timepoints following tracer injection. SUVmax and TBR for the bladder are excluded from the plot. Data values available in Supplemental Table 1.

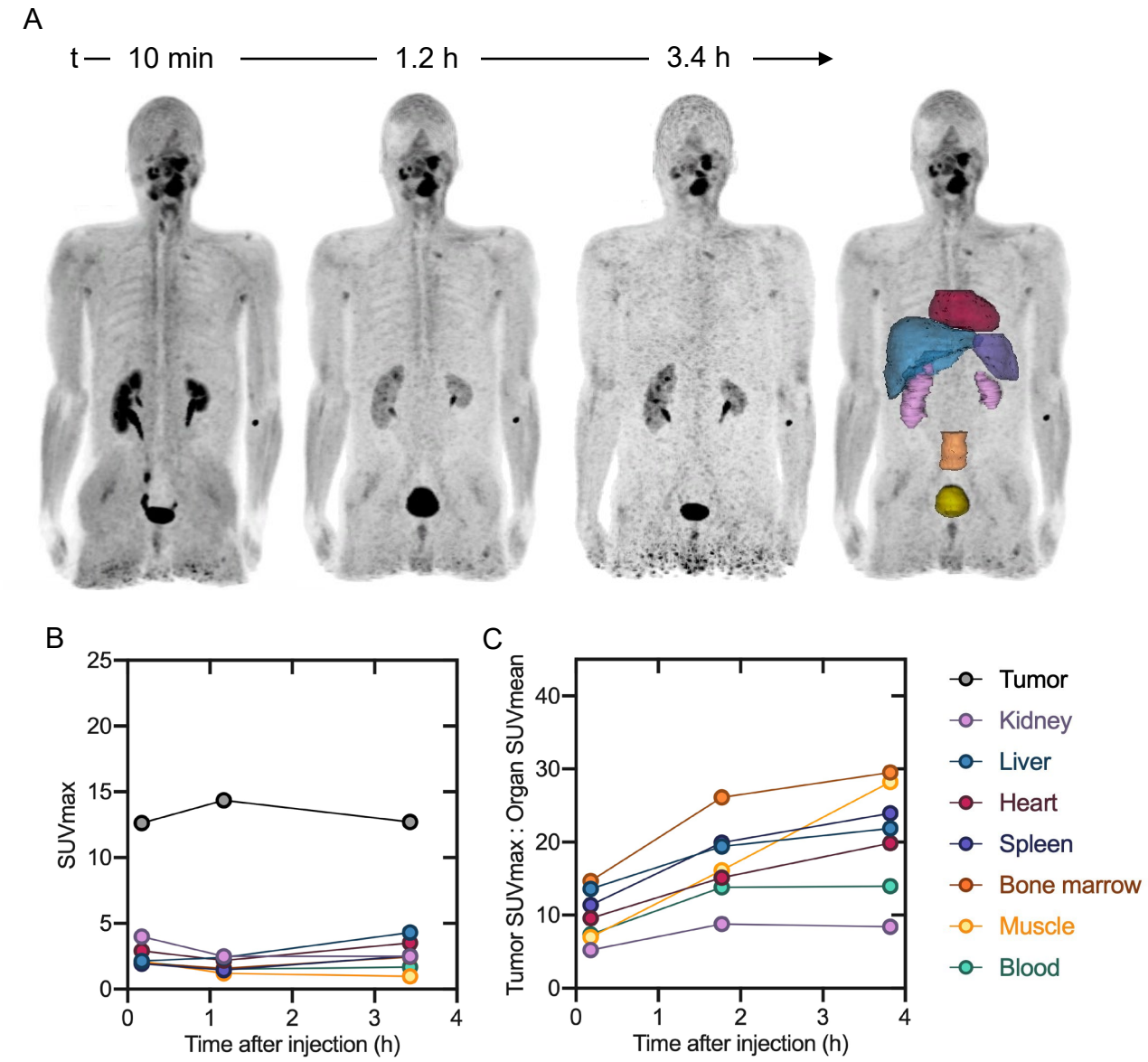

Supplemental Figure 3| Patient 4 A) ^{68}Ga-FAPI-46 MIP and delineated organs for dose calculations, B) SUVmax at three timepoints following tracer injection and C) TBR at three timepoints following tracer injection. SUVmax and TBR for the bladder are excluded from the plot. Data values available in Supplemental Table 1.

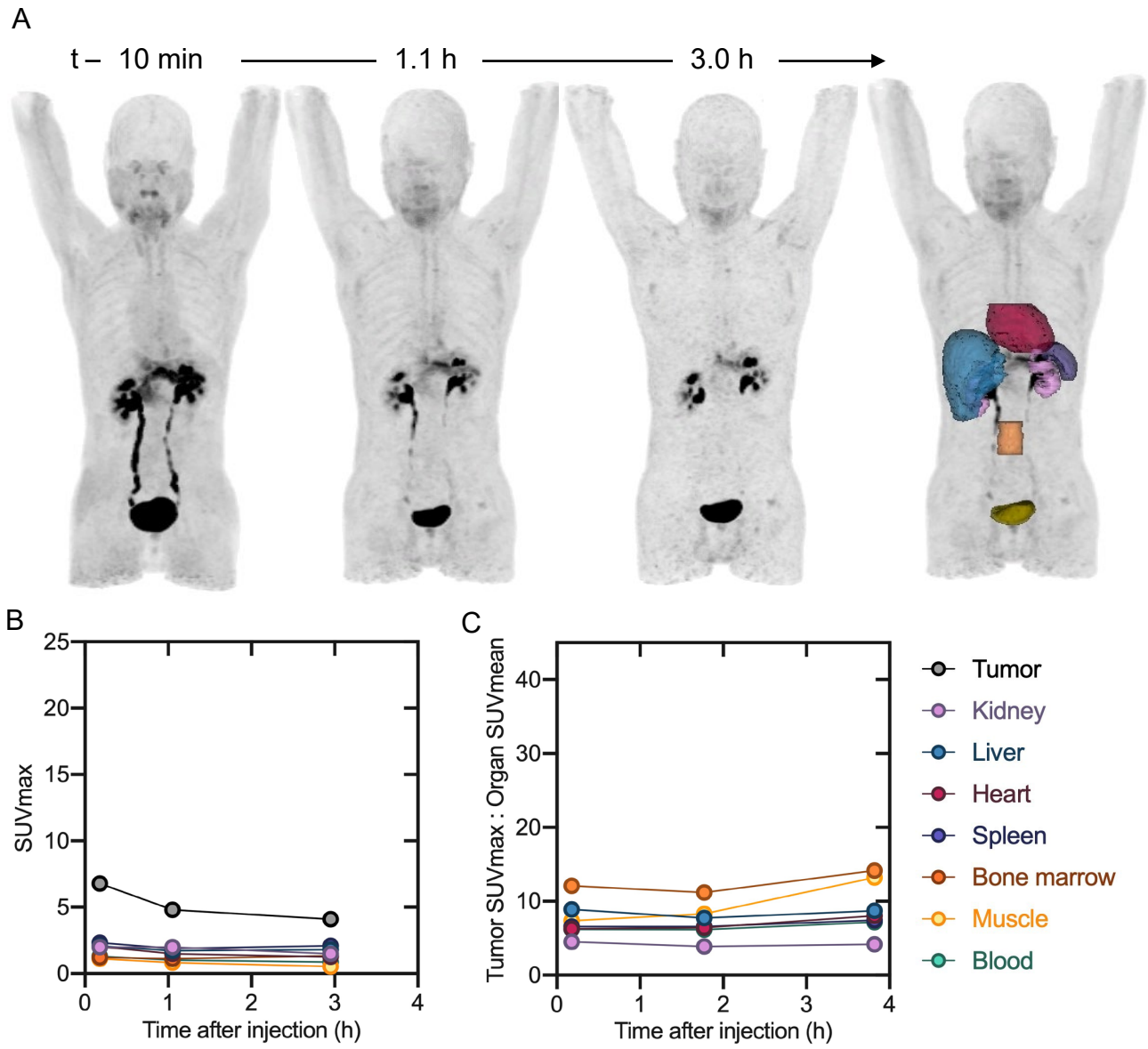

Supplemental Figure 4| Patient 6 A) ^{68}Ga-FAPI-46 MIP and delineated organs for dose calculations, B) SUVmax at three timepoints following tracer injection and C) TBR at three timepoints following tracer injection. SUVmax and TBR for the bladder are excluded from the plot. Data values available in Supplemental Table 1.

Supplemental Table 1 | Individual patient SUV ratios, SUVmax, and SUVmean values at three time points following ^{68}Ga-FAPI-46 administration

Patient 1

		11 minutes	1.8 hrs	3.8 hrs
SUVmax tumor: SUVmean organ	T : Liver	5.84	8.68	10.27
	T : Kidney	11.65	13.75	13.03
	T : Blood	14.53	19.11	15.40
	T : Muscle	16.30	23.88	23.77
	T: Heart	14.20	19.52	20.85
	T : Spleen	11.94	15.78	16.13
	T : Marrow	27.99	34.90	35.66
	T: Uterus	9.92	7.69	8.11
	T: Bladder	1.15	4.00	2.06
SUVmax	Tumor	18.75	18.15	13.55
	Liver	18.09	9.94	6.85
	Kidney	2.00	2.00	1.50
	Blood	1.45	1.20	1.16
	Muscle	1.64	1.20	1.14
	Heart	2.82	1.93	3.25
	Spleen	2.61	2.35	2.54
	Marrow	1.70	1.60	1.68
	Uterus	3.21	4.38	4.01
	Bladder	60.42	13.24	19.99
SUVmean	Tumor	5.61	3.52	2.18
	Liver	3.21	2.09	1.32
	Kidney	1.61	1.32	1.04
	Blood	1.29	0.95	0.88
	Muscle	1.15	0.76	0.57
	Heart	1.32	0.93	0.65
	Spleen	1.57	1.15	0.84
	Marrow	0.67	0.52	0.38
	Uterus	1.89	2.36	1.67
	Bladder	16.26	4.54	6.59

Patient 2

		13 minutes	1.1 hrs	3.3 hrs
SUVmax tumor: SUVmean organ	T : Liver	8.54	12.25	15.91
	T : Kidney	9.45	11.27	11.80
	T : Blood	13.67	17.33	23.12
	T : Muscle	13.16	20.19	32.11
	T: Heart	16.01	21.61	28.43
	T : Spleen	15.06	19.34	20.40
	T : Marrow	20.66	25.87	34.68
	T: Bladder	1.89	0.93	0.95
SUVmax	Tumor	17.77	18.37	17.34
	Liver	5.91	4.80	6.57
	Kidney	3.00	2.50	2.50
	Blood	1.61	1.35	1.53
	Muscle	1.66	1.20	0.97
	Heart	3.62	2.34	2.23
	Spleen	2.40	2.31	3.16
	Marrow	1.69	1.55	1.82
	Bladder	59.00	48.37	63.10
SUVmean	Tumor	3.79	3.95	3.63
	Liver	2.08	1.50	1.09
	Kidney	1.88	1.63	1.47
	Blood	1.30	1.06	0.75
	Muscle	1.35	0.91	0.54
	Heart	1.11	0.85	0.61
	Spleen	1.18	0.95	0.85
	Marrow	0.86	0.71	0.50
	Bladder	9.41	19.67	18.34

Patient 3

		11 minutes	1.0 hrs	3.0 hrs
SUVmax tumor: SUVmean organ	T : Liver	21.70	17.34	17.02
	T : Kidney	9.70	8.85	7.24
	T : Blood	13.85	10.55	9.80
	T : Muscle	10.69	8.55	9.90
	T: Heart	14.72	12.41	13.11
	T : Spleen	19.14	17.11	17.32
	T : Marrow	31.89	26.38	30.31
	T: Uterus	9.27	4.69	4.29
	T: Bladder	1.30	1.16	1.00
SUVmax	Tumor	21.05	12.66	9.70
	Liver	13.63	9.15	3.83
	Kidney	4.00	2.50	2.50
	Blood	2.06	1.41	1.61
	Muscle	2.47	2.07	1.79
	Heart	3.27	2.16	2.73
	Spleen	2.33	1.46	1.47
	Marrow	1.81	1.30	1.77
	Uterus	3.53	4.83	4.83
	Bladder	68.90	53.85	50.92
SUVmean	Tumor	2.80	2.37	1.66
	Liver	0.97	0.73	0.57
	Kidney	2.17	1.43	1.34
	Blood	1.52	1.20	0.99
	Muscle	1.97	1.48	0.98
	Heart	1.43	1.02	0.74
	Spleen	1.10	0.74	0.56
	Marrow	0.66	0.48	0.32
	Uterus	2.27	2.70	2.26
	Bladder	16.23	10.90	9.66

Patient 4

		10 minutes	1.2 hrs	3.4 hrs
SUVmax tumor: SUVmean organ	T : Liver	13.58	19.41	21.90
	T : Kidney	5.22	8.81	8.41
	T : Blood	7.39	13.81	13.96
	T : Muscle	6.98	16.13	28.22
	T: Heart	9.57	15.12	19.84
	T : Spleen	11.38	19.94	23.96
	T : Marrow	14.69	26.11	29.53
	T: Bladder	0.35	2.47	0.94
SUVmax	Tumor	12.63	14.36	12.70
	Liver	2.14	2.41	4.31
	Kidney	4.00	2.50	2.50
	Blood	2.06	1.52	1.68
	Muscle	2.12	1.19	0.96
	Heart	2.90	2.18	3.51
	Spleen	1.92	1.44	2.54
	Marrow	1.97	1.57	2.45
	Bladder	306.33	10.47	40.72
SUVmean	Tumor	3.58	4.16	3.28
	Liver	0.93	0.74	0.58
	Kidney	2.42	1.63	1.51
	Blood	1.71	1.04	0.91
	Muscle	1.81	0.89	0.45
	Heart	1.32	0.95	0.64
	Spleen	1.11	0.72	0.53
	Marrow	0.86	0.55	0.43
	Bladder	35.91	5.82	13.50

Patient 5

		17 minutes	1.4 hrs	3.1 hrs
SUVmax tumor: SUVmean organ	T : Liver	15.09	23.31	26.98
	T : Kidney	8.49	13.19	19.43
	T : Blood	9.70	17.93	25.76
	T : Muscle	9.76	18.40	29.40
	T: Heart	10.00	17.78	24.39
	T : Spleen	15.52	25.90	28.66
	T : Marrow	21.45	31.31	42.46
	T: Bladder	1.55	2.70	1.42
SUVmax	Tumor	16.30	20.98	22.93
	Liver	2.68	2.87	6.88
	Kidney	3.00	2.50	2.00
	Blood	2.10	1.76	1.39
	Muscle	2.22	1.71	2.01
	Heart	5.00	4.80	5.15
	Spleen	2.21	2.21	5.46
	Marrow	2.24	3.96	2.94
	Bladder	24.08	40.62	45.79
SUVmean	Tumor	5.16	4.54	5.00
	Liver	1.08	0.90	0.85
	Kidney	1.92	1.59	1.18
	Blood	1.68	1.17	0.89
	Muscle	1.67	1.14	0.78
	Heart	1.63	1.18	0.94
	Spleen	1.05	0.81	0.80
	Marrow	0.76	0.67	0.54
	Bladder	10.52	7.77	16.11

Patient 6

		11 minutes	1.1 hrs	3.0 hrs
SUVmax tumor: SUVmean organ	T : Liver	8.92	7.76	8.72
	T : Kidney	4.52	3.88	4.18
	T : Blood	6.22	6.17	7.19
	T : Muscle	7.37	8.29	13.23
	T: Heart	6.28	6.41	8.04
	T : Spleen	6.58	6.59	7.45
	T : Marrow	12.11	11.19	14.14
	T: Bladder	0.69	0.32	0.26
SUVmax	Tumor	6.78	4.81	4.10
	Liver	2.08	1.73	1.80
	Kidney	2.00	2.00	1.50
	Blood	1.31	1.01	0.87
	Muscle	1.11	0.82	0.54
	Heart	2.04	1.49	1.26
	Spleen	2.32	1.89	2.10
	Marrow	1.23	1.11	1.34
	Bladder	27.33	67.27	78.43
SUVmean	Tumor	2.30	1.70	1.09
	Liver	0.76	0.62	0.47
	Kidney	1.50	1.24	0.98
	Blood	1.09	0.78	0.57
	Muscle	0.92	0.58	0.31
	Heart	1.08	0.75	0.51
	Spleen	1.03	0.72	0.55
	Marrow	0.56	0.43	0.29
	Bladder	9.81	15.02	15.83

Supplemental Table 2 | Time-integrated activity coefficients (TIACs) per patient

$\%IA = A * \exp(-\lambda t)$							
	Heart	Bladder	Spleen	Marrow	Uterus	Kidney	Liver
Patient 1							
A (%)	1.590	7.550	1.480	2.220	0.136	1.140	6.740
λ (h^{-1})	0.840	1.720	0.812	0.720	0.447	0.776	1.010
TIAC (h)	0.019	0.044	0.018	0.031	0.003	0.015	0.067
Patient 2							
A (%)	2.020	3.720	1.510	3.620	N/A	2.830	6.030
λ (h^{-1})	0.965	0.316	1.160	8.100	N/A	0.969	1.020
TIAC (h)	0.021	0.118	0.013	0.004	N/A	0.029	0.059
Patient 3							
A (%)	1.280	4.400	0.196	1.780	0.130	1.880	1.840
λ (h^{-1})	0.965	0.992	1.020	0.932	0.544	1.380	0.868
TIAC (h)	0.013	0.044	0.002	0.019	0.002	0.014	0.021
Patient 4							
A (%)	1.540	9.800	0.291	2.920	N/A	2.250	1.970
λ (h^{-1})	0.960	2.900	0.947	0.940	N/A	1.400	0.827
TIAC (h)	0.016	0.034	0.003	0.031	N/A	0.016	0.024
Patient 5							
A (%)	2.050	8.170	0.260	2.560	N/A	1.620	1.970
λ (h^{-1})	0.893	1.950	0.873	0.716	N/A	0.857	0.726
TIAC (h)	0.023	0.042	0.003	0.036	N/A	0.019	0.027
Patient 6							
A (%)	1.680	7.290	0.520	2.540	N/A	2.700	2.380
λ (h^{-1})	0.989	0.964	0.958	0.891	N/A	1.100	0.821
TIAC (h)	0.017	0.076	0.005	0.029	N/A	0.025	0.029

Supplemental Table 3 | OLINDA dose reports

Patient 1

Target Organ	Alpha	Beta	Photon	Total	EDE Cont.	ED Cont.
Adrenals	0.00E+00	4.20E-03	2.53E-03	6.73E-03	0.00E+00	3.36E-05
Brain	0.00E+00	4.20E-03	1.17E-03	5.37E-03	0.00E+00	2.68E-05
Breasts	0.00E+00	4.20E-03	1.19E-03	5.39E-03	8.09E-04	2.70E-04
Gallbladder Wall	0.00E+00	4.20E-03	2.62E-03	6.82E-03	0.00E+00	0.00E+00
LLI Wall	0.00E+00	4.20E-03	2.40E-03	6.60E-03	0.00E+00	7.91E-04
Small Intestine	0.00E+00	4.20E-03	2.04E-03	6.24E-03	0.00E+00	3.12E-05
Stomach Wall	0.00E+00	4.20E-03	2.13E-03	6.33E-03	0.00E+00	7.59E-04
ULI Wall	0.00E+00	4.20E-03	2.22E-03	6.42E-03	0.00E+00	3.21E-05
Heart Wall	0.00E+00	9.87E-03	2.66E-03	1.25E-02	7.52E-04	0.00E+00
Kidneys	0.00E+00	1.30E-02	3.10E-03	1.61E-02	9.68E-04	8.06E-05
Liver	0.00E+00	2.02E-02	4.94E-03	2.51E-02	1.51E-03	1.26E-03
Lungs	0.00E+00	4.20E-03	1.82E-03	6.02E-03	7.22E-04	7.22E-04
Muscle	0.00E+00	4.20E-03	1.60E-03	5.80E-03	0.00E+00	2.90E-05
Ovaries	0.00E+00	4.20E-03	2.44E-03	6.64E-03	1.66E-03	1.33E-03
Pancreas	0.00E+00	4.20E-03	2.71E-03	6.91E-03	0.00E+00	3.45E-05
Red Marrow	0.00E+00	5.25E-03	1.86E-03	7.10E-03	8.53E-04	8.53E-04
Osteogenic Cells	0.00E+00	9.53E-03	1.81E-03	1.13E-02	3.40E-04	1.13E-04
Skin	0.00E+00	4.20E-03	9.89E-04	5.19E-03	0.00E+00	5.19E-05
Spleen	0.00E+00	9.87E-03	2.18E-03	1.20E-02	0.00E+00	6.02E-05
Thymus	0.00E+00	4.20E-03	1.76E-03	5.96E-03	0.00E+00	2.98E-05
Thyroid	0.00E+00	4.20E-03	1.32E-03	5.52E-03	1.66E-04	2.76E-04
Urinary Bladder Wall	0.00E+00	4.74E-02	8.24E-03	5.57E-02	3.34E-03	2.78E-03
Uterus	0.00E+00	1.25E-02	4.92E-03	1.75E-02	1.05E-03	8.73E-05
Total Body	0.00E+00	5.12E-03	2.12E-03	7.24E-03	0.00E+00	0.00E+00
Effective Dose Equivalent (mSv/MBq)					1.22E-02	
Effective Dose (mSv/MBq)						9.65E-03

Patient 2

Target Organ	Alpha	Beta	Photon	Total	EDE Cont.	ED Cont.
Adrenals	0.00E+00	3.76E-03	2.36E-03	6.13E-03	0.00E+00	3.06E-05
Brain	0.00E+00	3.76E-03	1.09E-03	4.85E-03	0.00E+00	2.42E-05
Breasts	0.00E+00	3.76E-03	1.08E-03	4.85E-03	7.27E-04	2.42E-04
Gallbladder Wall	0.00E+00	3.76E-03	2.47E-03	6.23E-03	0.00E+00	0.00E+00
LLI Wall	0.00E+00	3.76E-03	2.26E-03	6.02E-03	0.00E+00	7.23E-04
Small Intestine	0.00E+00	3.76E-03	2.12E-03	5.89E-03	0.00E+00	2.94E-05
Stomach Wall	0.00E+00	3.76E-03	1.94E-03	5.70E-03	0.00E+00	6.84E-04
ULI Wall	0.00E+00	3.76E-03	2.05E-03	5.81E-03	0.00E+00	2.91E-05
Heart Wall	0.00E+00	9.78E-03	2.45E-03	1.22E-02	7.34E-04	0.00E+00
Kidneys	0.00E+00	1.93E-02	3.40E-03	2.27E-02	1.36E-03	1.13E-04
Liver	0.00E+00	9.78E-03	3.20E-03	1.30E-02	7.79E-04	6.49E-04
Lungs	0.00E+00	3.76E-03	1.58E-03	5.34E-03	6.41E-04	6.41E-04
Muscle	0.00E+00	3.76E-03	1.52E-03	5.28E-03	0.00E+00	2.64E-05
Ovaries	0.00E+00	3.76E-03	2.32E-03	6.08E-03	1.52E-03	1.22E-03
Pancreas	0.00E+00	3.76E-03	2.47E-03	6.23E-03	0.00E+00	3.12E-05
Red Marrow	0.00E+00	6.90E-03	1.86E-03	8.76E-03	1.05E-03	1.05E-03
Osteogenic Cells	0.00E+00	8.53E-03	1.74E-03	1.03E-02	3.08E-04	1.03E-04
Skin	0.00E+00	3.76E-03	9.48E-04	4.71E-03	0.00E+00	4.71E-05
Spleen	0.00E+00	5.28E-03	1.52E-03	6.80E-03	4.08E-04	3.40E-05
Testes	0.00E+00	3.76E-03	1.58E-03	5.34E-03	0.00E+00	0.00E+00
Thymus	0.00E+00	3.76E-03	1.63E-03	5.39E-03	0.00E+00	2.69E-05
Thyroid	0.00E+00	3.76E-03	1.38E-03	5.14E-03	1.54E-04	2.57E-04
Urinary Bladder Wall	0.00E+00	4.42E-02	6.92E-03	5.11E-02	3.07E-03	2.56E-03
Uterus	0.00E+00	3.76E-03	2.94E-03	6.70E-03	0.00E+00	3.35E-05
Total Body	0.00E+00	4.60E-03	2.01E-03	6.61E-03	0.00E+00	0.00E+00
Effective Dose Equivalent (mSv/MBq)					1.08E-02	
Effective Dose (mSv/MBq)						8.55E-03

Patient 3

Target Organ	Alpha	Beta	Photon	Total	EDE Cont.	ED Cont.
Adrenals	0.00E+00	3.36E-03	2.05E-03	5.42E-03	0.00E+00	2.71E-05
Brain	0.00E+00	3.36E-03	1.20E-03	4.56E-03	0.00E+00	2.28E-05
Breasts	0.00E+00	3.36E-03	1.12E-03	4.48E-03	6.72E-04	2.24E-04
Gallbladder Wall	0.00E+00	3.36E-03	1.92E-03	5.28E-03	0.00E+00	0.00E+00
LLI Wall	0.00E+00	3.36E-03	2.31E-03	5.68E-03	0.00E+00	6.81E-04
Small Intestine	0.00E+00	3.36E-03	1.91E-03	5.27E-03	0.00E+00	2.64E-05
Stomach Wall	0.00E+00	3.36E-03	1.83E-03	5.19E-03	0.00E+00	6.23E-04
ULI Wall	0.00E+00	3.36E-03	2.05E-03	5.42E-03	0.00E+00	2.71E-05
Heart Wall	0.00E+00	7.58E-03	2.20E-03	9.79E-03	5.87E-04	0.00E+00
Kidneys	0.00E+00	1.34E-02	2.64E-03	1.60E-02	9.61E-04	8.01E-05
Liver	0.00E+00	4.17E-03	2.01E-03	6.18E-03	0.00E+00	3.09E-04
Lungs	0.00E+00	3.36E-03	1.59E-03	4.95E-03	5.94E-04	5.94E-04
Muscle	0.00E+00	3.36E-03	1.51E-03	4.87E-03	0.00E+00	2.44E-05
Ovaries	0.00E+00	3.36E-03	2.34E-03	5.71E-03	1.43E-03	1.14E-03
Pancreas	0.00E+00	3.36E-03	2.09E-03	5.45E-03	0.00E+00	2.72E-05
Red Marrow	0.00E+00	3.93E-03	1.72E-03	5.66E-03	6.79E-04	6.79E-04
Osteogenic Cells	0.00E+00	7.38E-03	1.74E-03	9.12E-03	2.74E-04	9.12E-05
Skin	0.00E+00	3.36E-03	9.55E-04	4.32E-03	0.00E+00	4.32E-05
Spleen	0.00E+00	4.34E-03	2.23E-03	6.57E-03	3.94E-04	3.29E-05
Thymus	0.00E+00	3.36E-03	1.68E-03	5.04E-03	0.00E+00	2.52E-05
Thyroid	0.00E+00	3.36E-03	1.34E-03	4.70E-03	1.41E-04	2.35E-04
Urinary Bladder Wall	0.00E+00	3.99E-02	7.14E-03	4.71E-02	2.82E-03	2.35E-03
Uterus	0.00E+00	1.07E-02	4.47E-03	1.52E-02	9.11E-04	7.59E-05
Total Body	0.00E+00	3.71E-03	1.63E-03	5.34E-03	0.00E+00	0.00E+00
Effective Dose Equivalent (mSv/MBq)					9.46E-03	
Effective Dose (mSv/MBq)						7.34E-03

Patient 4

Target Organ	Alpha	Beta	Photon	Total	EDE Cont.	ED Cont.
Adrenals	0.00E+00	2.96E-03	1.66E-03	4.62E-03	0.00E+00	2.31E-05
Brain	0.00E+00	2.96E-03	9.09E-04	3.87E-03	0.00E+00	1.93E-05
Breasts	0.00E+00	2.96E-03	8.59E-04	3.82E-03	5.73E-04	1.91E-04
Gallbladder Wall	0.00E+00	2.96E-03	1.66E-03	4.62E-03	0.00E+00	0.00E+00
LLI Wall	0.00E+00	2.96E-03	1.80E-03	4.76E-03	2.86E-04	5.71E-04
Small Intestine	0.00E+00	2.96E-03	1.67E-03	4.63E-03	0.00E+00	2.31E-05
Stomach Wall	0.00E+00	2.96E-03	1.44E-03	4.40E-03	0.00E+00	5.28E-04
ULI Wall	0.00E+00	2.96E-03	1.59E-03	4.55E-03	0.00E+00	2.27E-05
Heart Wall	0.00E+00	7.56E-03	1.87E-03	9.43E-03	5.66E-04	0.00E+00
Kidneys	0.00E+00	1.07E-02	2.05E-03	1.27E-02	7.64E-04	6.36E-05
Liver	0.00E+00	2.98E-03	1.51E-03	4.48E-03	0.00E+00	2.24E-04
Lungs	0.00E+00	2.96E-03	1.21E-03	4.16E-03	5.00E-04	5.00E-04
Muscle	0.00E+00	2.96E-03	1.20E-03	4.16E-03	0.00E+00	2.08E-05
Ovaries	0.00E+00	2.96E-03	1.84E-03	4.80E-03	1.20E-03	9.61E-04
Pancreas	0.00E+00	2.96E-03	1.70E-03	4.66E-03	0.00E+00	2.33E-05
Red Marrow	0.00E+00	5.23E-03	1.45E-03	6.68E-03	8.01E-04	8.01E-04
Osteogenic Cells	0.00E+00	6.59E-03	1.40E-03	7.99E-03	2.40E-04	7.99E-05
Skin	0.00E+00	2.96E-03	7.59E-04	3.72E-03	0.00E+00	3.72E-05
Spleen	0.00E+00	3.21E-03	1.38E-03	4.59E-03	0.00E+00	2.29E-05
Testes	0.00E+00	2.96E-03	1.28E-03	4.24E-03	0.00E+00	0.00E+00
Thymus	0.00E+00	2.96E-03	1.31E-03	4.27E-03	0.00E+00	2.13E-05
Thyroid	0.00E+00	2.96E-03	1.15E-03	4.11E-03	1.23E-04	2.06E-04
Urinary Bladder Wall	0.00E+00	3.12E-02	5.02E-03	3.62E-02	2.17E-03	1.81E-03
Uterus	0.00E+00	2.96E-03	2.28E-03	5.24E-03	3.14E-04	2.62E-05
Total Body	0.00E+00	3.37E-03	1.49E-03	4.86E-03	0.00E+00	0.00E+00
Effective Dose Equivalent (mSv/MBq)					7.54E-03	
Effective Dose (mSv/MBq)						6.18E-03

Patient 5

Target Organ	Alpha	Beta	Photon	Total	EDE Cont.	ED Cont.
Adrenals	0.00E+00	2.53E-03	2.28E-03	4.80E-03	0.00E+00	2.40E-05
Brain	0.00E+00	2.53E-03	1.36E-03	3.89E-03	0.00E+00	1.94E-05
Breasts	0.00E+00	2.53E-03	1.26E-03	3.79E-03	5.69E-04	1.90E-04
Gallbladder Wall	0.00E+00	2.53E-03	2.30E-03	4.83E-03	0.00E+00	0.00E+00
LLI Wall	0.00E+00	2.53E-03	2.54E-03	5.07E-03	0.00E+00	6.09E-04
Small Intestine	0.00E+00	2.53E-03	2.39E-03	4.92E-03	0.00E+00	2.46E-05
Stomach Wall	0.00E+00	2.53E-03	2.09E-03	4.62E-03	0.00E+00	5.54E-04
ULI Wall	0.00E+00	2.53E-03	2.28E-03	4.81E-03	0.00E+00	2.41E-05
Heart Wall	0.00E+00	8.92E-03	2.67E-03	1.16E-02	6.95E-04	0.00E+00
Kidneys	0.00E+00	7.56E-03	1.93E-03	9.49E-03	5.70E-04	4.75E-05
Liver	0.00E+00	3.29E-03	1.97E-03	5.26E-03	3.15E-04	2.63E-04
Lungs	0.00E+00	2.53E-03	1.75E-03	4.28E-03	5.13E-04	5.13E-04
Muscle	0.00E+00	2.53E-03	1.73E-03	4.26E-03	0.00E+00	2.13E-05
Ovaries	0.00E+00	2.53E-03	2.61E-03	5.14E-03	1.29E-03	1.03E-03
Pancreas	0.00E+00	2.53E-03	2.37E-03	4.90E-03	0.00E+00	2.45E-05
Red Marrow	0.00E+00	5.01E-03	2.02E-03	7.03E-03	8.44E-04	8.44E-04
Osteogenic Cells	0.00E+00	5.97E-03	2.03E-03	8.00E-03	2.40E-04	8.00E-05
Skin	0.00E+00	2.53E-03	1.11E-03	3.64E-03	0.00E+00	3.64E-05
Spleen	0.00E+00	2.71E-03	1.64E-03	4.35E-03	0.00E+00	2.18E-05
Testes	0.00E+00	2.53E-03	1.84E-03	4.37E-03	0.00E+00	0.00E+00
Thymus	0.00E+00	2.53E-03	1.93E-03	4.46E-03	0.00E+00	2.23E-05
Thyroid	0.00E+00	2.53E-03	1.73E-03	4.26E-03	1.28E-04	2.13E-04
Urinary Bladder Wall	0.00E+00	3.48E-02	6.18E-03	4.10E-02	2.46E-03	2.05E-03
Uterus	0.00E+00	2.53E-03	3.12E-03	5.65E-03	3.39E-04	2.82E-05
Total Body	0.00E+00	2.77E-03	1.46E-03	4.23E-03	0.00E+00	0.00E+00
Effective Dose Equivalent (mSv/MBq)					7.96E-03	
Effective Dose (mSv/MBq)						6.64E-03

Patient 6

Target Organ	Alpha	Beta	Photon	Total	EDE Cont.	ED Cont.
Adrenals	0.00E+00	4.05E-03	1.87E-03	5.92E-03	0.00E+00	2.96E-05
Brain	0.00E+00	4.05E-03	9.63E-04	5.02E-03	0.00E+00	2.51E-05
Breasts	0.00E+00	4.05E-03	9.22E-04	4.98E-03	7.46E-04	2.49E-04
Gallbladder Wall	0.00E+00	4.05E-03	1.86E-03	5.92E-03	0.00E+00	0.00E+00
LLI Wall	0.00E+00	4.05E-03	2.13E-03	6.18E-03	0.00E+00	7.42E-04
Small Intestine	0.00E+00	4.05E-03	1.88E-03	5.93E-03	0.00E+00	2.97E-05
Stomach Wall	0.00E+00	4.05E-03	1.60E-03	5.65E-03	0.00E+00	6.78E-04
ULI Wall	0.00E+00	4.05E-03	1.78E-03	5.83E-03	0.00E+00	2.92E-05
Heart Wall	0.00E+00	8.99E-03	2.01E-03	1.10E-02	6.60E-04	0.00E+00
Kidneys	0.00E+00	1.61E-02	2.74E-03	1.88E-02	1.13E-03	9.41E-05
Liver	0.00E+00	4.51E-03	2.01E-03	6.52E-03	0.00E+00	3.26E-04
Lungs	0.00E+00	4.05E-03	1.30E-03	5.36E-03	6.43E-04	6.43E-04
Muscle	0.00E+00	4.05E-03	1.34E-03	5.40E-03	0.00E+00	2.70E-05
Ovaries	0.00E+00	4.05E-03	2.16E-03	6.21E-03	1.55E-03	1.24E-03
Pancreas	0.00E+00	4.05E-03	1.92E-03	5.97E-03	0.00E+00	2.99E-05
Red Marrow	0.00E+00	5.67E-03	1.57E-03	7.24E-03	8.69E-04	8.69E-04
Osteogenic Cells	0.00E+00	8.09E-03	1.51E-03	9.59E-03	2.88E-04	9.59E-05
Skin	0.00E+00	4.05E-03	8.34E-04	4.89E-03	0.00E+00	4.89E-05
Spleen	0.00E+00	5.64E-03	1.78E-03	7.42E-03	4.45E-04	3.71E-05
Testes	0.00E+00	4.05E-03	1.50E-03	5.56E-03	0.00E+00	0.00E+00
Thymus	0.00E+00	4.05E-03	1.40E-03	5.45E-03	0.00E+00	2.73E-05
Thyroid	0.00E+00	4.05E-03	1.23E-03	5.28E-03	1.58E-04	2.64E-04
Urinary Bladder Wall	0.00E+00	5.08E-02	7.59E-03	5.84E-02	3.50E-03	2.92E-03
Uterus	0.00E+00	4.05E-03	2.89E-03	6.95E-03	4.17E-04	3.47E-05
Total Body	0.00E+00	4.68E-03	1.96E-03	6.64E-03	0.00E+00	0.00E+00
Effective Dose Equivalent (mSv/MBq)					1.04E-02	
Effective Dose (mSv/MBq)						8.44E-03